INVESTIGATION OF THE EFFECT OF COOLING RATE ON ATOMIC STRUCTURE OF LIQUID CALCIUM: A MOLECULAR DYNAMICS SIMULATION STUDY

Murat Celtek[1], Sedat Sengul[2], Unal Domekeli[2]

[1]*Faculty of Education, Trakya University, 22030, Edirne – TURKEY*
[2]*Dept. of Physics, Trakya University, 22030, Edirne – TURKEY*

Abstract

In this study, the evolution of the atomic structure of liquid calcium (Ca) cooled with different cooling rates (10-0.02 K/ps) was investigated using the classical molecular dynamics simulation method. The embedded atom method many body potentials, which are widely preferred in molecular dynamics simulations, were used to describe the interactions between Ca atoms in the system. Volume temperature curves, pair distribution functions, structure factor and Honeycutt-Andersen method were used to examine the changes in the atomic structure of liquid Ca during the cooling process. A good agreement was observed between the pair distribution functions and structure factors curves calculated from molecular dynamics simulations for liquid Ca and the experimental and other molecular dynamics simulation results in the literature. Current findings have shown that liquid Ca, which is cooled faster, exhibits properties unique to amorphous structures at lower temperatures. On the other hand, it has been found that when the system is given more time to cool (or is cooled more slowly), crystal nucleation begins and the size of this nucleation increases, eventually making the system transition from a liquid to a crystalline structure. According to the results of Honeycutt-Andersen pair analysis method, 1551, 1431 and 1541 bonded pairs are more common in amorphous systems, while 1441 and 1661 bonded pairs are more popular in crystalline structures. It is believed that the results of the study will provide useful information to the literature about the development of the atomic structure of Ca, which has a wide range of uses in our lives.

Keywords: Calcium, Molecular Dynamics Simulations, Honeycutt-Andersen Method, Embedded atom method.

INTRODUCTION

With the developing technology and increasing demand, many materials are needed today and feverish work is carried out to produce them. However, producing new materials and conducting research and development studies on them can be both laborious and expensive. As such, it is of great importance to be able to explain the physical properties of that material at the atomic scale in accurate, fast, reliable and inexpensive ways [1]. Today, with the spread of supercomputers and the parallel development of the software industry, the adverse effects of experimental studies such as time, manpower, and cost can be alleviated to some extent [2–4]. The most commonly used methods in the literature to investigate the physical properties of materials; quantum-based molecular dynamics (MD) simulation methods and classical MD simulation methods based on the solution of Newtonian equations of motion [5]. Although quantum MD simulations produce reliable results close to experimental results, they have some disadvantages such as slow computation and working with very few atoms. Because of these disadvantages, classical MD simulation methods are preferred because they are cheaper, can work with millions of atoms, require less computing power, have a more easily understandable theoretical background, can produce reliable results with accurate modeling. Thus, in our study, we focused on the effect of cooling rate on the evolution of the atomic structure of liquid calcium (Ca) during the cooling process by taking these advantages of classical MD simulations. We used the embedded atom method (EAM) potential to express the interactions between Ca atoms in the system. It has been reported in previous studies that the EAM potential produces successful results in explaining the structural properties of Ca under different conditions [1, 6].

EXPOSITION

According to the EAM model, the total energy rising from the interactions between atoms in a system with N atoms is defined as,

$$E_i = F_\alpha \left[\sum_{j \neq i} \rho_{\alpha\beta}(r_{ij}) \right] + \frac{1}{2} \sum_{j \neq i} \phi_{\alpha\beta}(r_{ij}), \qquad (1)$$

where $\phi_{\alpha\beta}(r_{ij})$ is the pair-interaction energy representing the repulsive interactions between two atoms. The second term F_α is the embedding energy, which depends on the charge density ρ_i, which includes attractive interactions. All simulations throughout the cooling process were performed using the DL_POLY_2.0 open-source simulation program [7]. During the simulations, NPT isothermal isobaric ensemble was used under 0 GPa pressure. Pressure and temperature were controlled with a Berendsen barostat and thermostat. Periodic boundary conditions were applied to all directions of the cell, which consists of a total of 13,500 Ca atoms. Velocity form of the Verlet algorithm was used to solve the equations of motion, and the time step was taken as 1 fs. In order to guarantee the liquid structure, the system was equilibrated by holding it at 500 ps at 1700 K, which is high enough than the experimental melting point ($T_m^{exp} = 1113$ K [8]) of Ca. Then, the liquid system was cooled with different cooling rates (γ_1=10, γ_2=5, γ_3=1, γ_4=0.1 and γ_5=0.02 Kps^{-1}) from 1700 K to 200 K with ΔT= 50 K intervals. The temperature-dependent variation of the volume of the system per atom (V-T) obtained by the five cooling rates is shown in Figure 1. In the high-temperature region (900 K-1700 K) for the five cooling rates, the volume of the system changes linearly and their curves almost overlap each other. This indicates that the atoms have enough mobility in this region and move fast enough that they can easily adapt to the current temperature. At low temperatures, the volume behaves in different slopes and shapes depending on the cooling rate of the system. The volume change is continuous under fast cooling rates of γ_1=10 Kps^{-1} and γ_2=5 Kps^{-1} and shows no indication of liquid-solid phase transition. The mobile atoms in the liquid system tend to move more slowly under these cooling rates because the viscosity of the liquid

constantly increases as the temperature drops [9]. However, in V-T curves obtained for slower cooling rates of γ_3=1 Kps^{-1}, γ_4=0.1 Kps^{-1} and γ_5=0.02 Kps^{-1}, an evident discontinuity is observed at 600 K, 700 K and 750 K, respectively, this indicates that a first-order phase transition has occurred in the system. These results show that the slower a system is cooled, the higher its transition temperature (crystallization temperature). This phenomenon has also been observed in many other studies. Unlike the others, at a cooling rate of γ_4=0.1 Kps^{-1}, two different changes are observed in the V-T curve between 600 K and 750 K, which will be discussed later with different analysis methods.
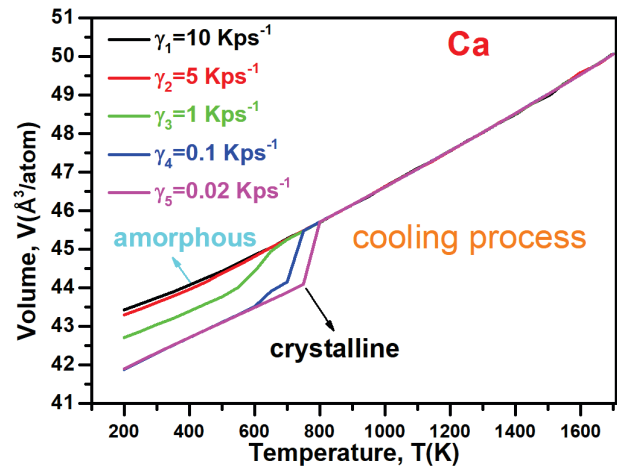
Fig. 1. *Temperature-dependent evolution of volume for five cooling rates.*

In MD simulations, the pair distribution function (PDF or g(r)) is one of the most preferred methods to characterize the local structure of the system and to obtain information about the distribution of atoms. It is also the probability to find another atom at a distance r from a central one. It can be expressed as [10, 11]:

$$g(r) = \frac{V}{N^2} \left\langle \sum_i \frac{n_i(r)}{4\pi r^2 \Delta r} \right\rangle. \qquad (2)$$

The liquid structure factor (S(q)), calculated from the Fourier transform of g(r), is shown in Figure 2 along with orbital-free ab-initio MD (OF-AIMD) simulation [12] and experimental [13] results. The liquid g(r) obtained from the EAM-MD simulations is in excellent agreement with both the experimental (excluding first peak height difference) and OF-AIMD simulation results. This is one of the

indications that the chosen potential accurately and reliably describes the interactions between Ca atoms.
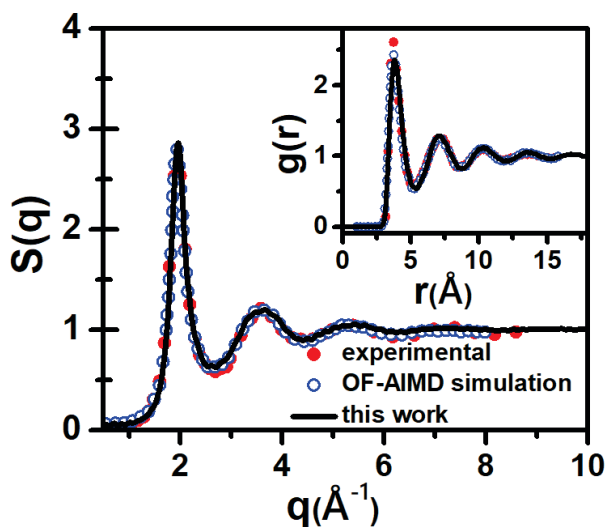
Fig. 2. *Comparison of S(q) (1100 K) calculated for liquid Ca with experimental and OF-AIMD simulation results (1113 K). The inset depicts liquid g(r)'s.*

Figure 3 presents a comparison of g(r)'s calculated at different temperatures for various cooling rates (γ_1=10 Kps^{-1}, γ_3=1 Kps^{-1}, and γ_5=0.02 Kps^{-1}). We did not include the results of other cooling rates in this graph, because it may cause visual pollution. The g(r)'s of the system cooled using the three cooling rates at 1000 K and 1500 K are very similar and they produce wider and lower peaks as in the g(r) of the liquid systems. This supports the fact that the atoms in the system can move fast enough at these temperatures, as discussed above. When the temperature is reduced to 600 K, g(r)'s calculated for the cooling rates of γ_1=10 Kps^{-1} and γ_3=1 Kps^{-1} are similar to each other and exhibit specific behavior to liquid structures, while g(r) obtained from γ_5=0.02 Kps^{-1} shows sharp and distinct peaks specific to crystalline structures. It is seen from the figure that the g(r)'s at 300 K exhibits different behavior for the three cooling rates. The first peak height of g(r), calculated from the cooling rate of γ_1=10 Kps^{-1}, increases and the widths of the main peaks decrease, while splitting is observed at the second maximum of the g(r) curve. These findings show that the short-range and medium-range order develops in the faster cooled system and there is a transition from liquid to the amorphous structure during cooling. Moreover, the main peaks of g(r) calculated for γ_3=1 Kps^{-1} cooling rate produce peaks with the same positions as the main peaks of g(r) calculated for γ_5=0.02 Kps^{-1}, but they have softer peaks. The g(r)'s obtained by the γ_5=0.02 Kps^{-1} shows peaks specific to the bcc crystalline structures, thus the results of slower cooling with the γ_3=1 Kps^{-1} suggest that apart from the presence of bcc clusters in the system, other clusters develop in the system.
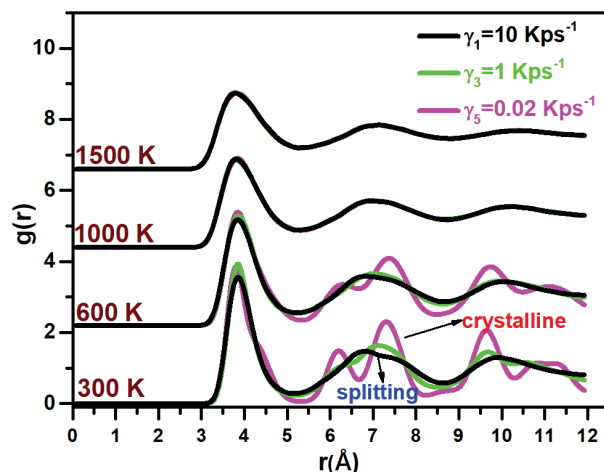
Fig. 3. *Comparison of g(r)'s calculated at different temperatures for cooling rates of γ_1=10 Kps^{-1}, γ_3=1 Kps^{-1}, and γ_5=0.02 Kps^{-1}.*

Although g(r) gives useful information about the atomic structure development of the system, it does not provide information about the microstructure of the system. Honeycutt-Andersen (HA) bond index [14–17] and Voronoi tessellation (VT) [18, 19] analysis are generally used to obtain detailed information about the local structure of the system. In the HA method, pairs of atoms and their local surroundings are characterized by integers *ijkl*. According to this technique, 1551 bonded pairs represent ideal icosahedra, 1541 and 1431 bonded pairs defective icosahedra. 1421 bonded pairs represent face-centered cubic (fcc) crystal structures, 1422+1421 bonded pairs represent the hexagonal closed-packed (hcp), 1661 and 1441 bonded pairs represent body-centered cubic (bcc) crystal structures. The diagrammatic nomenclature and configurations of the different HA bonded pairs most commonly seen in our study are shown in Figure 4.
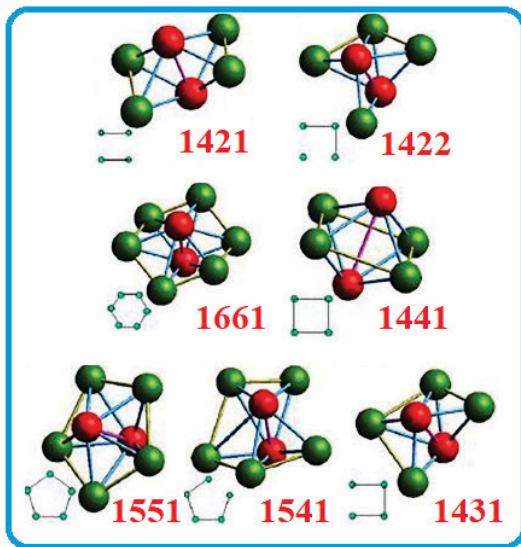
Fig. 4. *Schematic representation of the most common HA bonded pairs indices. The red and green balls represent the root pair atoms and their common neighbors.*

The fractions of the most common bonded pairs according to the HA analysis results of the data obtained for the three cooling rates during the cooling process are shown in Figure 5 as a function of temperature. It can be seen from the figures that the bonded pairs 1551, 1431 and 1541 are the most dominant in the high-temperature regions. These bonded pairs continue to dominate even at low temperatures for a cooling rate of $\gamma_1=10$ Kps^{-1}. This is an indication that the system transitions from liquid to the amorphous structure at low temperatures during the rapid cooling process. Another important observation is that while 1551 bonded pairs tend to increase from 1700 K to 700 K, they tend to decrease below 700 K, and a slight increase is observed in the fraction of bonded pairs representing crystal structures in this process. This shows that during the rapid cooling process, crystal nucleation started to occur at low temperatures, but these nuclei did not have the opportunity to grow because there was not enough time. Looking at the results shown in Figure 4(b) for the $\gamma_3=1$ Kps^{-1} cooling rate, it can be seen that the results are quite similar to the results for $\gamma_1=10$ Kps^{-1} at high (600 K and above) temperatures. However, a sudden decrease is observed in the fraction of popular bonded pairs around 600 K, while a sudden increase is observed in 1421 bonded pairs representing fcc crystal structures as well as 1441 and 1661 bonded pairs representing bcc crystal structures. It shows that this system has

transitioned from a liquid structure to a polycrystalline one dominated by atoms in bcc crystal order. In order to provide a visual overview of this explanation, we show the atoms in bcc, hcp and fcc crystal order at 300 K in the inset of the figure.
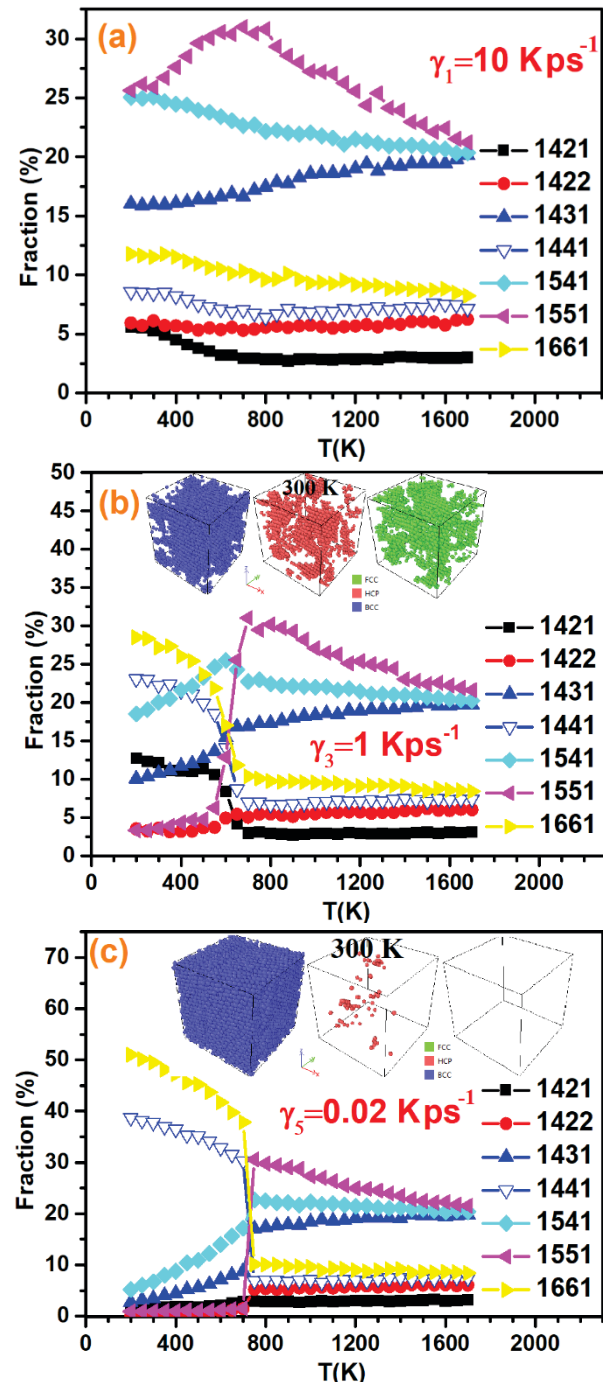
Fig. 5. *Temperature-dependent evolutions of fractions of some HA bonded pairs obtained for (a) $\gamma_1=10$ Kps^{-1}, (b) $\gamma_3=1$ Kps^{-1}, and (c) $\gamma_5=0.02$ Kps^{-1} cooling rate during the cooling process.*

The fractions of HA bonded pairs at high temperatures of the system cooled with a

cooling rate of γ_5=0.02 Kps^{-1} are similar to that of other cooling rates, but around 750 K a sharp decrease is observed in all popular pairs, while a sharp increase is observed in the fraction of 1661 and 1441 bonded pairs. This shows that, unlike the others, the liquid system transitions to the solid phase with a bcc crystal order of around 750 K. It is possible to confirm this from the snapshots of the simulation boxes at 300 K given in the inset of the figure. In addition, these observations and findings are consistent with the results presented and discussed in Figure 3. All these results show that the selected cooling rate has an important role in the evolution of the atomic structure during the rapid solidification process. In order to clarify the abnormal behavior observed between 750K and 600K in the V-T curve obtained for the γ_4=0.1 Kps^{-1} cooling rate in Figure 1, the snapshots of crystal and other ordered atoms at these temperatures and the calculated g(r)'s of them are shown together in Figure 6. From the snapshots, it is seen that the number of atoms with bcc, hcp and fcc order in the system at 750 K is almost non-existent. The g(r) curves on the side supports this results. It is understood from the figure that the other bonded pairs, which are mostly in liquid and amorphous structures in the system at this temperature, are in the majority because the total g(r) curve of the system and the g(r) curve of the other pairs overlap.
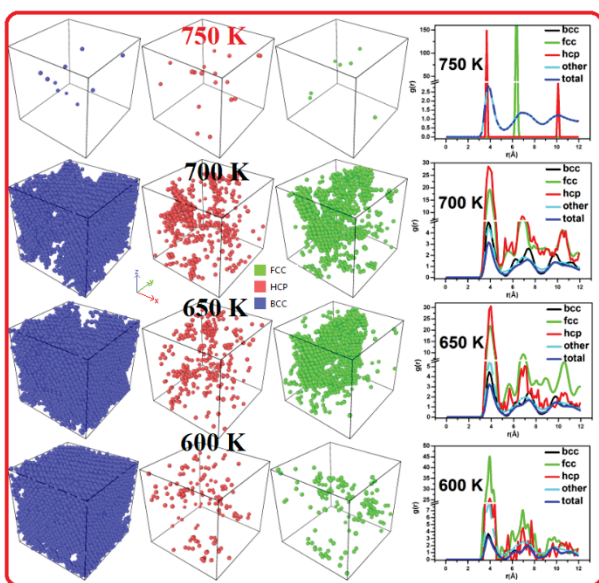
***Fig. 6.** Snapshots of bcc, hcp and fcc atoms at different temperatures for a cooling rate of γ_4=0.1 Kps^{-1}, and the g(r) curves calculated for them.*

When the temperature is reduced to 700 K, it can be seen from the snapshots that atoms in bcc order fill most of the system, but also exist the atoms in hcp and fcc order at a non-negligible portion. A similar scene is observed at 650 K, except for the increase in the number of atoms in fcc crystal order. Current findings indicate that the system stabilizes in a polycrystalline order in this temperature range. It is possible to observe this from the relationship between the g(r) curves. The total g(r) curves reflect the characteristics of all other atoms, mostly bcc atoms, in their respective proportions. Finally, when the temperature is reduced by 600 K, it is seen that the bcc order is dominant in the system and there is a noticeable decrease in the number of atoms with hcp and fcc order. In addition, it is seen that the total g(r) curve and the g(r) curves calculated only for bcc atoms almost overlap. These findings show that the system transitions from the polycrystalline order to the bcc crystalline order at 600 K and explain the reason for the abnormal behavior observed in the V-T curves of γ_4=0.1 Kps^{-1} at these temperatures.

CONCLUSION

In the present study, the evolution of the atomic structure of liquid Ca during the rapid solidification process was investigated by the MD simulation method using five different cooling rates and EAM potential. The g(r) and S(q) curves calculated from the EAM-MD simulations show excellent agreement with the experimental and OF-AIMD simulation results previously reported in the literature. It has been observed that the time given for the cooling of the system during the cooling process has an important role in the evolution of the atomic structure of the system. For faster cooling rates (γ_1=10 Kps^{-1} and γ_2=5 Kps^{-1}), no phase transition was observed in the system and the liquid system cooled at these rates evolved into an amorphous structure. In the second maximum of the g(r)'s, a splitting, typical for amorphous structures, is observed. According to HA analysis results, 1551, 1541 and 1431 bonded pairs were found to be popular, showing the presence of icosahedral and defective icosahedral order in the system at these cooling rates. When the system was cooled with slower

cooling rates ($\gamma_3=1$, $\gamma_4=0.1$ and $\gamma_5=0.02$ Kps^{-1}), a liquid-solid first-order phase transition occurred in the system at temperatures below the melting point. HA analysis shows that the system cooled with $\gamma_3=1$ Kps^{-1} cooling rate is balanced in polycrystalline order, while at cooling rates of $\gamma_4=0.1$ and $\gamma_5=0.02$ Kps^{-1}, bcc crystal order dominates at low temperatures. We believe that the results will contribute to a better understanding of the evolution of the atomic structure of liquid Ca during the rapid solidification process.

REFERENCE

[1] Celtek M. Investigation of Heating Process of Pure Calcium Element by Molecular Dynamics Simulation Method. BEU J Sci 2021; 10: 803–815.

[2] Celik FA, Yildiz A. Pressure effect on the icosahedral order of Pd50Si50 alloy: A molecular dynamics study. Mater Today Commun 2020; 25: 101454.

[3] Celtek M. An in-depth investigation of the microstructural evolution and dynamic properties of Zr77Rh23 metallic liquids and glasses: A molecular dynamics simulation study. J Appl Phys 2022; 132: 035902.

[4] Atila A, Kbirou M, Ouaskit S, et al. On the presence of nanoscale heterogeneity in Al70Ni15Co15 metallic glass under pressure. J Non Cryst Solids 2020; 550: 120381.

[5] Çeltek M, Güder V. Sıvı Vanadyumun Kristalizasyon Sürecine Soğutma Oranı Etkisinin Moleküler Dinamik Benzetim Metodu ile İncelenmesi. Erzincan Üniversitesi Fen Bilim Enstitüsü Derg 2020; 13: 730–745.

[6] Celtek M, Sengul S, Domekeli U. A molecular dynamics simulation study on the structural evolution of liquid calcium under high pressure. In: *International Scientific Conference*. 2021, pp. 265–270.

[7] Smith W, Forester TR. DL_POLY_2.0: A general-purpose parallel molecular dynamics simulation package. J Mol Graph 1996; 14: 136–141.

[8] Kittel C. *Introduction to Solid State Physics*. New York: John Wiley & Sons Inc., 1986.

[9] Ozdemir Kart S, Tomak M, Uludogan M, et al. Structural, thermodynamical, and transport properties of undercooled binary Pd-Ni alloys. Mater Sci Eng A 2006; 435–436: 736–744.

[10] Kbirou M, Trady S, Hasnaoui A, et al. Cooling rate dependence and local structure in aluminum monatomic metallic glass. Philos Mag 2017; 97: 2753–2771.

[11] Celtek M, Sengul S, Domekeli U, et al. Dynamical and structural properties of metallic liquid and glass Zr48Cu36Ag8Al8 alloy studied by molecular dynamics simulation. J Non Cryst Solids 2021; 566: 120890.

[12] Rio BG del, González LE. Orbital free ab initio simulations of liquid alkaline earth metals: from pseudopotential construction to structural and dynamic properties. J Phys Condens Matter 2014; 26: 465102.

[13] Waseda Y. *The Structure of Non-Crystalline Materials-Liquids and Amorphous Solids*. New York: London: McGraw-Hill, 1981.

[14] Celtek M. Atomic structure of Cu60Ti20Zr20 metallic glass under high pressures. Intermetallics 2022; 143: 107493.

[15] Honeycutt JD, Andersen HC. Molecular Dynamics Study of Melting and Freezing of Small Lennard- Jones Clusters. J Phys Chem 1987; 91: 4950–4963.

[16] Guder V, Sengul S, Celtek M, et al. Pressure dependent evolution of microstructures in Pd80Si20 bulk metallic glass. J Non Cryst Solids 2022; 576: 121290.

[17] Sengul S, Domekeli U, Celtek M. Effect of Cooling Rate on the Atomic Structure Of Al75Co255 Metallic Glass. J Tech Univ Gabrovo 2021; 63: 76–80.

[18] Voronoi G. New Parametric Applications Concerning the Theory of Quadratic Forms - Second Announcement. J Reine Angew Math 1908; 134: 198–287.

[19] Celtek M, Domekeli U, Sengul S, et al. Effects of Ag or Al addition to CuZr-based metallic alloys on glass formation and structural evolution: a molecular dynamics simulation study. Intermetallics 2021; 128: 107023.